AC

FISIST/4-95/CFIF
TKU-HEP 95/01

Searching for Signatures of Supersymmetry at B-Factories

G. C. Branco[1], G. C. Cho[2] *, Y. Kizukuri[2] †, and N. Oshimo[3] ‡

[1] *Departamento de Física and CFIF/UTL, Instituto Superior Técnico*
Av. Rovisco Pais, 1096 Lisboa Codex, Portugal
[2] *Department of Physics, Tokai University*
1117 Kita-Kaname, Hiratsuka 259-12, Japan
[3] *GTAE/CFIF, Instituto Superior Técnico*
Av. Rovisco Pais, 1096 Lisboa Codex, Portugal

Yoshiki Kizukuri passed away on November 4, 1994. His three coauthors will miss him as a collaborator and a friend.

Abstract

We analyze the predictions for CP asymmetries in B^0-meson decays within the framework of the supersymmetric standard model (SSM). It is pointed out that owing to sizable new contributions to B_d^0-$\bar{B}_d^0$ and K^0-$\bar{K}^0$ mixings, the experimentally allowed range for the CP-violating phase δ of the Cabibbo-Kobayashi-Maskawa matrix may be different from the one obtained in the standard model (SM). This has important effects on the allowed values of CP asymmetries in B^0-meson decays and on their correlations. We calculate the ratio R of the SSM and the SM contributions to the B_d^0-$\bar{B}_d^0$ mixing parameter x_d and discuss in detail the ranges of R and δ which are consistent with the experimental values of x_d and the CP violation parameter ϵ for K^0-$\bar{K}^0$ mixing. The CP asymmetries are predicted to have values different from the SM predictions in sizable regions of parameter space. We also discuss the SSM predictions for B_s^0-$\bar{B}_s^0$ mixing.

---

*Research Fellow of the Japan Society for the Promotion of Science.

†Supported by Grant-in-Aid for Scientific Research from the Ministry of Education, Science and Culture, contract number 6640409.

‡Address after April 1, 1995: Department of Physics, Ochanomizu University, Otsuka 2-1-1, Bunkyo-ku, Tokyo 112, Japan.

1 Introduction

The measurement of CP asymmetries in neutral B-meson decays is one of the main tasks of B-factories, which will subject the standard model (SM) and in particular its mechanism of CP violation to an important test [1]. In this paper, we study in detail the predictions for CP asymmetries in B^0-meson decays, within the framework of the supersymmetric standard model (SSM) [2], with the aim of finding possible signatures of supersymmetry.

Both in the SM and in the SSM, CP asymmetries in B^0-meson decays can measure $\sin 2\phi_\alpha$, $\sin 2\phi_\beta$, and $\sin 2\phi_\gamma$, where ϕ_α, ϕ_β, and ϕ_γ denote the angles of the Cabibbo-Kobayashi-Maskawa (CKM) unitarity triangle. These CP asymmetries are expressed in terms of $|V_{us}|$, $|V_{ub}/V_{cb}|$, and $\cos\delta$, with V_{ij} denoting a CKM matrix element and δ being the CP-violating phase in the standard parametrization [3] of the CKM matrix. Since the SSM does not give new contributions to tree-level decay rates of strange particles and B-mesons, the evaluation of the CKM matrix elements V_{us}, V_{ub}, and V_{cb} from experiments is the same in the SSM and the SM. However, the allowed range of $\cos\delta$ in the SSM can differ from the SM range. Therefore, the CP asymmetries could be predicted differently by the SM and the SSM.

The reason why the SSM may give a different allowed range for $\cos\delta$ stems from the fact that in the SSM there are new contributions [4, 5] to the B_d^0-$\bar{B}_d^0$ mixing parameter x_d, as well as to the CP violation parameter ϵ in the K-meson sector. Indeed, recently we have pointed out [6] that for sizable ranges of its parameters, the SSM gives significant new contributions to B_d^0-$\bar{B}_d^0$ and K^0-$\bar{K}^0$ mixings, of strength comparable to that of the SM contributions. These relatively large SSM contributions arise from the box diagrams (see Fig. 1) mediated by charginos and up-type squarks and those mediated by charged Higgs bosons and up-type quarks.

We first reexamine the SSM contributions to B_d^0-$\bar{B}_d^0$ and K^0-$\bar{K}^0$ mixings in detail, paying special attention to their dependence on SSM parameters. For definiteness, the analysis is made within the framework of grand unification theories coupled to $N = 1$ supergravity. We calculate the ratio R of the SSM and the SM contributions for B_d^0-$\bar{B}_d^0$ mixing, and show that for sizable regions of parameter space, R is enhanced to be around two or even larger. It is also shown that the SSM contribution to ϵ is determined by R.

We next discuss in detail the ranges of R and $\cos\delta$ which are consistent with the experimental values of ϵ and x_d. Having determined the allowed range of $\cos\delta$,

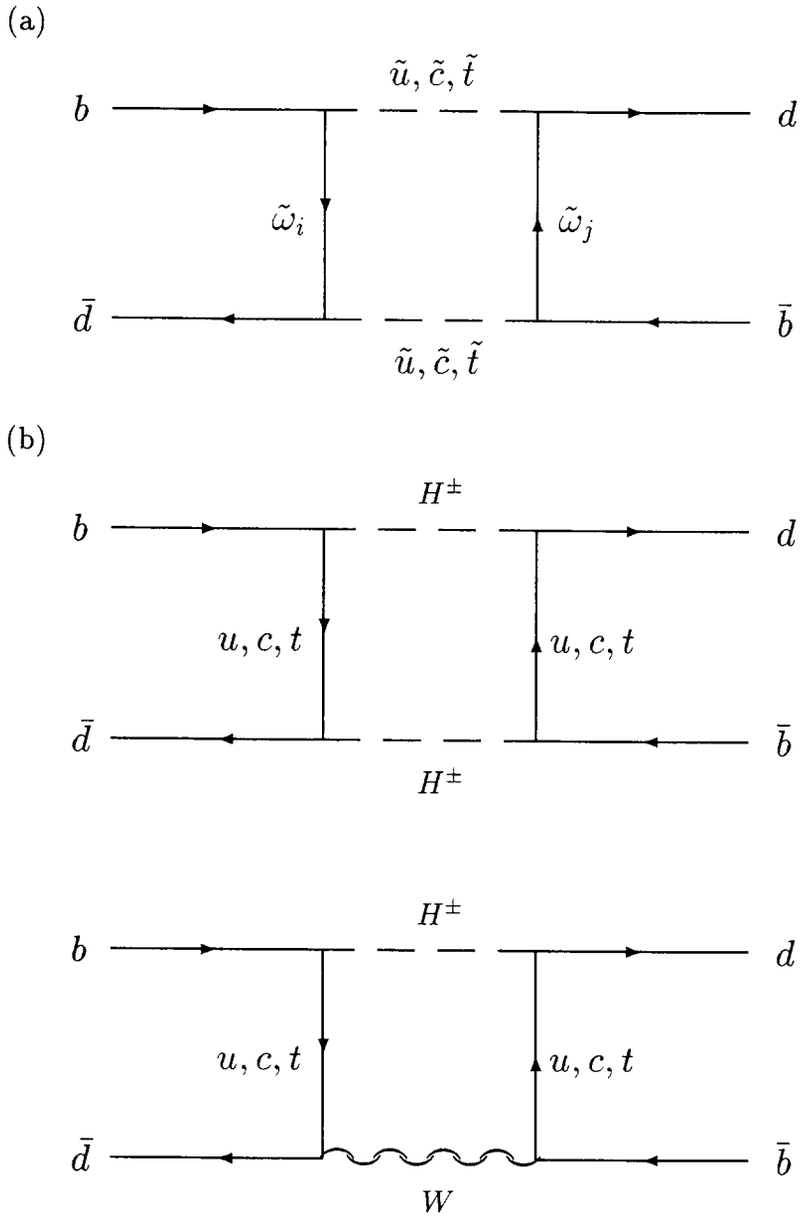

Figure 1: The Feynman diagrams for B_d^0-$\bar{B}_d^0$ mixing: (a) The chargino contribution, (b) The charged Higgs boson contribution.

we derive the predictions of the SSM for CP asymmetries in B^0-meson decays and also for the ratio x_s/x_d, with x_s denoting the B_s^0-$\bar{B}_s^0$ mixing parameter.

This paper is organized as follows: In sect. 2 we briefly review the mechanisms which induce flavor-changing neutral current (FCNC) processes in the SSM. In sect. 3 we discuss the SSM contributions to B_d^0-$\bar{B}_d^0$ and K^0-$\bar{K}^0$ mixings and explore SSM parameter regions where sizable enhancements are obtained. In sect. 4 we consider the constraints on $\cos\delta$ and R, and discuss the predictions for the CP asymmetries and B_s^0-$\bar{B}_s^0$ mixing in both the SM and the SSM. The analysis of this section is to a great extent independent of the details of the SSM, so that the results are applicable to other models. Our conclusions are presented in sect. 5. In an appendix we list some of the equations necessary for our analyses.

2 Interactions

The SSM predicts new interactions for quarks. A quark interacts with a squark $\tilde{q}$ and a chargino $\tilde{\omega}$, a neutralino $\tilde{\chi}$, or a gluino $\tilde{g}$, and with another quark and a charged Higgs boson $H^\pm$. In all these interactions, when expressed in terms of particle mass eigenstates, a quark can couple to a squark or to another quark in a different generation. However, sizable new contributions to FCNC processes can only be expected from the interactions mediated by the charginos and/or the charged Higgs bosons [7, 8]. Therefore, we neglect the interactions mediated by the gluinos and the neutralinos throughout this paper.

The charginos are the mass eigenstates of the SU(2) charged gauginos and the charged higgsinos. Their mass matrix is given by

$$M^- = \begin{pmatrix} \tilde{m}_2 & -\frac{1}{\sqrt{2}}gv_1 \\ -\frac{1}{\sqrt{2}}gv_2 & m_H \end{pmatrix}, \tag{1}$$

where v_1 and v_2 are the vacuum expectation values of the Higgs bosons, and $\tilde{m}_2$ and m_H respectively denote the SU(2) gaugino mass and the higgsino mass parameter. In the ordinary scheme for gaugino mass generation, $\tilde{m}_2$ is smaller than or around the gravitino mass $m_{3/2}$. If the SU(2)×U(1) symmetry is broken through radiative corrections, $\tan\beta$ ($\equiv v_2/v_1$) $\gtrsim 1$ holds and the magnitude of m_H is at most of order of $m_{3/2}$. The chargino mass eigenstates are obtained by diagonalizing the matrix M^- as

$$C_R^\dagger M^- C_L = \mathrm{diag}(\tilde{m}_{\omega 1}, \tilde{m}_{\omega 2}) \quad (\tilde{m}_{\omega 1} < \tilde{m}_{\omega 2}), \tag{2}$$

where C_R and C_L are unitary matrices.

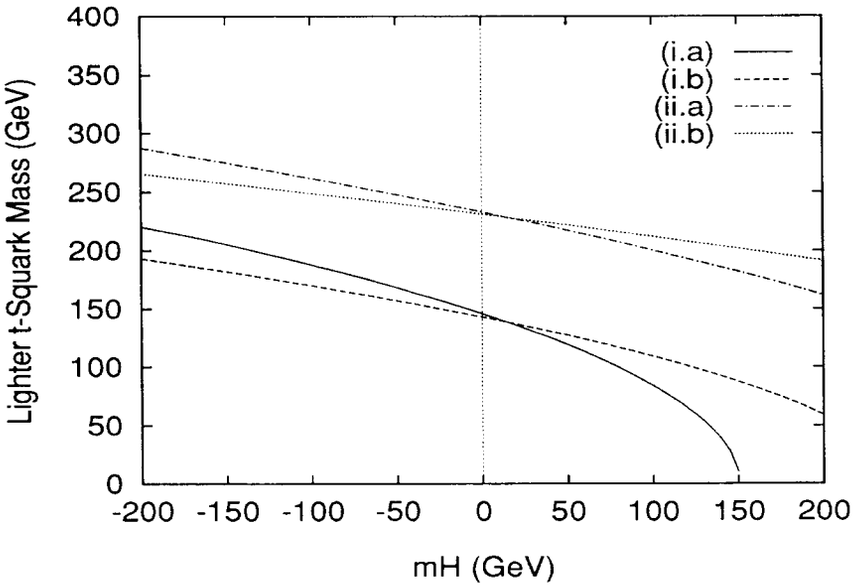

Figure 2: The lighter t-squark mass. The values of $\tilde{m}_Q$ and $\tan\beta$ for curves (i.a)–(ii.b) are given in table 1. The other parameters are set for $\tilde{m}_U = am_{3/2} = \tilde{m}_Q$ and $|c| = 0.3$.

There is generation mixing both among quark fields and among squark fields. Since the left-handed squarks and the right-handed ones are also mixed, the mass-squared matrices for the up-type squarks M_U^2 is expressed by a 6×6 matrix:

$$
\begin{aligned}
M_U^2 &= \begin{pmatrix} M_{U11}^2 & M_{U12}^2 \\ M_{U21}^2 & M_{U22}^2 \end{pmatrix}; \qquad (3) \\
M_{U11}^2 &= \cos 2\beta(\frac{1}{2} - \frac{2}{3}\sin^2\theta_W)M_Z^2 + \tilde{m}_Q^2 + (1+c)m_U m_U^\dagger + dm_D m_D^\dagger, \\
M_{U22}^2 &= \frac{2}{3}\cos 2\beta \sin^2\theta_W M_Z^2 + \tilde{m}_U^2 + (1+2c)m_U^\dagger m_U, \\
M_{U12}^2 &= M_{U21}^{2\dagger} = \cot\beta m_H m_U + a^* m_{3/2} m_U,
\end{aligned}
$$

where m_U and m_D denote the mass matrices of the up-type and down-type quarks. The mass parameters $m_{3/2}$, $\tilde{m}_Q$, $\tilde{m}_U$ and the dimensionless constants a, c, d come from the terms in the SSM lagrangian which break supersymmetry softly: $\tilde{m}_Q$ and $\tilde{m}_U$ are determined by the gravitino and gaugino masses and $\tilde{m}_Q \simeq \tilde{m}_U \sim m_{3/2}$; a is related to the breaking of local supersymmetry and its absolute value is constrained to be less than 3 at the grand unification scale; c and d are related to radiative corrections to the squark masses. At the electroweak energy scale, a is of order unity and $-c = 0.1 - 1$. The value of d is also of order unity, so that $dm_D m_D^\dagger$ can be neglected compared to $(1+c)m_U m_U^\dagger$ in eq. (3).

	(i.a)	(i.b)	(ii.a)	(ii.b)
$\tilde{m}_Q$ (GeV)	200	200	300	300
$\tan\beta$	1.2	2.0	1.2	2.0

Table 1: The values of $\tilde{m}_Q$ and $\tan\beta$ for curves (i.a)–(ii.b) in Fig. 2.

The quark mass matrices are diagonalized by unitary matrices as

$$\begin{aligned} U_L^U m_U U_R^{U\dagger} &= \mathrm{diag}(m_u, m_c, m_t) \quad (\equiv \bar{m}_U), \\ U_L^D m_D U_R^{D\dagger} &= \mathrm{diag}(m_d, m_s, m_b) \quad (\equiv \bar{m}_D). \end{aligned} \tag{4}$$

The CKM matrix is given by $V = U_L^U U_L^{D\dagger}$. The squark mixings among different generations in eq. (3) are, neglecting $dm_D m_D^\dagger$, removed by the 6×6 matrix

$$\begin{pmatrix} U_L^U & 0 \\ 0 & U_R^U \end{pmatrix}, \tag{5}$$

leaving only the left-handed and right-handed squarks mixed in each flavor. As a result, the generation mixings in the lagrangian between the down-type quarks and the up-type squarks in mass eigenstates are also described by the CKM matrix. The mixings between the left-handed and right-handed squarks can be neglected for the first two generations because of the smallness of the corresponding quark masses. The masses of the left-handed squarks $\tilde{u}_L, \tilde{c}_L$ and the right-handed squarks $\tilde{u}_R, \tilde{c}_R$ are given by

$$\begin{aligned} \tilde{M}_{uL}^2 = \tilde{M}_{cL}^2 &= \tilde{m}_Q^2 + \cos 2\beta(\frac{1}{2} - \frac{2}{3}\sin^2\theta_W)M_Z^2, \\ \tilde{M}_{uR}^2 = \tilde{M}_{cR}^2 &= \tilde{m}_U^2 + \frac{2}{3}\cos 2\beta \sin^2\theta_W M_Z^2. \end{aligned} \tag{6}$$

For the third generation, the large t-quark mass leads to an appreciable mixing between $\tilde{t}_L$ and $\tilde{t}_R$. The mass-squared matrix for the t-squarks becomes

$$M_t^2 = \begin{pmatrix} \tilde{M}_{uL}^2 + (1-|c|)m_t^2 & (\cot\beta m_H + a^* m_{3/2})m_t \\ (\cot\beta m_H^* + a m_{3/2})m_t & \tilde{M}_{uR}^2 + (1-2|c|)m_t^2 \end{pmatrix}. \tag{7}$$

The mass eigenstates of the t-squarks are obtained by diagonalizing the matrix M_t^2 as

$$S_t M_t^2 S_t^\dagger = \mathrm{diag}(\tilde{M}_{t1}^2, \tilde{M}_{t2}^2) \quad (\tilde{M}_{t1}^2 < \tilde{M}_{t2}^2), \tag{8}$$

where S_t is a unitary matrix.

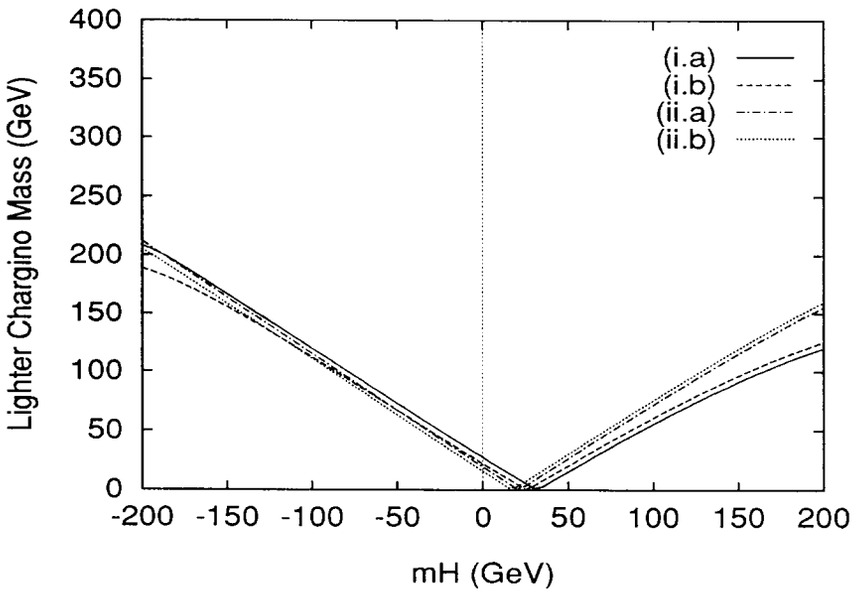

Figure 3: The lighter chargino mass. The values of $\tilde{m}_2$ and $\tan\beta$ for curves (i.a)–(ii.b) are given in table 2.

Experimentally there is a lower bound of 90 GeV [3] on the squark masses of the first two generations. Since the mass scale of these squarks is determined by $\tilde{m}_Q$ ($\simeq \tilde{m}_U$), this constraint is satisfied for $\tilde{m}_Q > 90$ GeV. If $\tilde{m}_Q$ is not much larger than this lower bound, the off-diagonal elements of M_t^2 in eq. (7) could be comparable with the diagonal elements because of the large t-quark mass, making one t-squark much lighter than the other squarks. In Fig. 2 we show the lighter t-squark mass as a function of the higgsino mass parameter m_H for $\tilde{m}_Q = 200$, 300 GeV and $\tan\beta = 1.2$, 2. The parameter values for each curve are listed in table 1. The other SSM parameters are set for $\tilde{m}_U = am_{3/2} = \tilde{m}_Q$ and $|c| = 0.3$. For the t-quark mass we use $m_t = 170$ GeV [9] throughout this paper. We see that the lighter t-squark can become light for $\tilde{m}_Q = 200$ GeV with a reasonable value of m_H. The t-squark may be as light as 45 GeV [3, 10]. In Fig. 3 we show the lighter chargino mass for $\tilde{m}_2 = 200$, 300 GeV and $\tan\beta = 1.2$, 2. The parameter values for each curve are listed in table 2. This mass does not depend much on $\tilde{m}_2$ nor $\tan\beta$. The parameter values which give $\tilde{m}_{\omega 1} \lesssim 45$ GeV are experimentally ruled out [3].

In general, the SSM parameters have complex values. If the magnitudes of their physical complex phases are of order unity, the electric dipole moment of the neutron is predicted to have a large value. Its experimental limits then lead to a lower bound of about 1 TeV on the squark masses [11]. In this case, the

	(i.a)	(i.b)	(ii.a)	(ii.b)
$\tilde{m}_2$ (GeV)	200	200	300	300
$\tan\beta$	1.2	2.0	1.2	2.0

Table 2: The values of $\tilde{m}_2$ and $\tan\beta$ for curves (i.a)–(ii.b) in Fig. 3.

SSM does not give any sizable new contributions to FCNC processes. We assume hereafter real values for the parameters other than the SM parameters, so that the constraints from the electric dipole moment of the neutron can be ignored.

The interaction lagrangians for the down-type quarks can now be written explicitly in terms of particle mass eigenstates. For the chargino–squark–quark interactions, we obtain [8]

$$
\begin{aligned}
L_{\tilde{\omega}} = & i\frac{g}{\sqrt{2}}\sum_{i=1}^{2} \\
& [(\tilde{u}_1^\dagger, \tilde{c}_1^\dagger, \sum_{k=1}^{2} S_{tk1}\tilde{t}_k^\dagger)V\bar{\omega}_i\{\sqrt{2}C_{R1i}^*(\frac{1-\gamma_5}{2}) + \frac{\bar{m}_D}{M_W}\frac{C_{L2i}^*}{\cos\beta}(\frac{1+\gamma_5}{2})\}\begin{pmatrix} d \\ s \\ b \end{pmatrix} \\
& -(\tilde{u}_2^\dagger, \tilde{c}_2^\dagger, \sum_{k=1}^{2} S_{tk2}\tilde{t}_k^\dagger)\frac{\bar{m}_U}{M_W}\frac{C_{R2i}^*}{\sin\beta}V\bar{\omega}_i(\frac{1-\gamma_5}{2})\begin{pmatrix} d \\ s \\ b \end{pmatrix}] \\
& +\text{h.c.},
\end{aligned}
\tag{9}
$$

where $\tilde{u}_1 = \tilde{u}_L$, $\tilde{u}_2 = \tilde{u}_R$ and $\tilde{c}_1 = \tilde{c}_L$, $\tilde{c}_2 = \tilde{c}_R$. In our approximation $\bar{m}_U$ and $\bar{m}_D$ should be taken as $\mathrm{diag}(0,0,m_t)$ and $\mathrm{diag}(0,0,m_b)$, respectively. The lagrangian for the charged Higgs boson–quark–quark interactions is obtained without approximation as [5]

$$
\begin{aligned}
L_{H^\pm} = & \frac{g}{\sqrt{2}} \\
& H^+(\bar{u},\bar{c},\bar{t})\{\cot\beta\frac{\bar{m}_U}{M_W}V(\frac{1-\gamma_5}{2}) + \tan\beta V\frac{\bar{m}_D}{M_W}(\frac{1+\gamma_5}{2})\}\begin{pmatrix} d \\ s \\ b \end{pmatrix} \\
& +\text{h.c.}.
\end{aligned}
\tag{10}
$$

The parameters which determine the FCNC processes induced by the charged Higgs boson interactions, other than the SM parameters, are only the charged Higgs boson mass $M_{H^\pm}$ and $\tan\beta$.

We can see from eq. (9) that the chargino interactions with the t-squarks and the down-type quarks contain the Yukawa interactions whose strengths are, owing

to a large value of the t-quark mass, as strong as those of the gauge interactions. By the same reason, the strengths of the charged Higgs boson interactions with the t-quark and the down-type quarks in eq. (10) are comparable with the gauge interaction strengths. The contributions to FCNC processes by these interactions could thus be as large as those by the standard W-boson interactions.

3 B^0-$\bar{B}^0$ and K^0-$\bar{K}^0$ mixings

The interactions in the SSM add new contributions to B^0-$\bar{B}^0$ and K^0-$\bar{K}^0$ mixings through box diagrams as shown in Fig.1. There are diagrams where charginos and up-type squarks are exchanged and diagrams where up-type quarks are exchanged together with either only charged Higgs bosons or charged Higgs bosons and W-bosons.

The effective lagrangian for B_d^0-$\bar{B}_d^0$ mixing induced by the chargino interactions becomes [6, 7]

$$L^C_{B_d^0} = \frac{1}{8M_W^2}\left(\frac{g^2}{4\pi}\right)^2 (V_{31}^* V_{33})^2 \\ [A_V^C \bar{d}\gamma^\mu \frac{1-\gamma_5}{2} b \bar{d}\gamma_\mu \frac{1-\gamma_5}{2} b + A_S^C \bar{d}\frac{1+\gamma_5}{2} b \bar{d}\frac{1+\gamma_5}{2} b], \tag{11}$$

$$A_n^C = \sum_{i,j}\sum_{k,l}[F_n^C(3,k;3,l;i,j) + F_n^C(1,k;1,l;i,j) \\ - F_n^C(1,k;3,l;i,j) - F_n^C(3,k;1,l;i,j)] \quad (n = V, S),$$

$$F_V^C(a,k;b,l;i,j) = \frac{1}{4} G^{(a,k)i} G^{(a,k)j*} G^{(b,l)i*} G^{(b,l)j} Y_1(r_{(a,k)}, r_{(b,l)}, s_i, s_j),$$
$$F_S^C(a,k;b,l;i,j) = H^{(a,k)i} G^{(a,k)j*} G^{(b,l)i*} H^{(b,l)j} Y_2(r_{(a,k)}, r_{(b,l)}, s_i, s_j),$$

where a, b are generation indices, and i, j and k, l stand respectively for the two charginos and the two squarks in each flavor. Coupling constants $G^{(a,k)i}$, $H^{(a,k)i}$ are derived from eq. (9) as

$$G^{(1,1)i} = G^{(2,1)i} = \sqrt{2} C_{R1i}^*, \quad G^{(1,2)i} = G^{(2,2)i} = 0,$$
$$G^{(3,k)i} = \sqrt{2} C_{R1i}^* S_{tk1} - \frac{C_{R2i}^* S_{tk2}}{\sin\beta}\frac{m_t}{M_W},$$
$$H^{(1,1)i} = H^{(2,1)i} = \frac{C_{L2i}^*}{\cos\beta}\frac{m_b}{M_W}, \quad H^{(1,2)i} = H^{(2,2)i} = 0, \tag{12}$$
$$H^{(3,k)i} = \frac{C_{L2i}^* S_{tk1}}{\cos\beta}\frac{m_b}{M_W}.$$

The functions Y_1 and Y_2 are defined in the appendix, their arguments being given by

$$\begin{aligned} r_{(1,1)} &= r_{(2,1)} = \frac{\tilde{M}^2_{uL}}{M^2_W}, \quad r_{(1,2)} = r_{(2,2)} = \frac{\tilde{M}^2_{uR}}{M^2_W}, \quad r_{(3,k)} = \frac{\tilde{M}^2_{tk}}{M^2_W}, \\ s_i &= \frac{\tilde{m}^2_{\omega i}}{M^2_W}. \end{aligned} \tag{13}$$

The unitarity of the CKM matrix has been used in eq. (11), and $L^C_{B^0_d}$ is proportional to $(V^*_{31}V_{33})^2$. The effective lagrangian $L^C_{B^0_d}$ contains a new quark operator proportional to A^C_S which is not yielded by the W-boson interactions. However, since A^C_S is suppressed by $(m_b/M_W)^2$ compared to A^C_V, this quark operator can be neglected unless $\tan\beta$ is much larger than one. The chargino interactions similarly induce B^0_s-$\bar{B}^0_s$ and K^0-$\bar{K}^0$ mixings. The effective lagrangians $L^C_{B^0_s}$ and $L^C_{K^0}$ for these mixings are obtained from eq. (11) by replacing $(V^*_{31}V_{33})^2$ with $(V^*_{32}V_{33})^2$ and $(V^*_{31}V_{32})^2$, respectively, putting $A^C_S = 0$ for $L^C_{K^0}$, and changing the quark operators appropriately.

For the charged Higgs boson interactions, the effective lagrangian for B^0_d-$\bar{B}^0_d$ mixing is given by [5, 6]

$$\begin{aligned} L^H_{B^0_d} = &\frac{1}{8M^2_W}\left(\frac{g^2}{4\pi}\right)^2 \sum_{a,b} V^*_{a1}V_{a3}V^*_{b1}V_{b3} \\ &[F^H_V(a;b)\bar{d}\gamma^\mu \frac{1-\gamma_5}{2} b \bar{d}\gamma_\mu \frac{1-\gamma_5}{2} b + F^H_S(a;b)\bar{d}\frac{1+\gamma_5}{2} b \bar{d}\frac{1+\gamma_5}{2} b], \end{aligned} \tag{14}$$

$$\begin{aligned} F^H_V(a;b) &= \frac{1}{4\tan^4\beta} s_a s_b Y_1(r_H, r_H, s_a, s_b) \\ &\quad + \frac{1}{2\tan^2\beta} s_a s_b Y_1(1, r_H, s_a, s_b) - \frac{2}{\tan^2\beta}\sqrt{s_a s_b} Y_2(1, r_H, s_a, s_b), \\ F^H_S(a;b) &= \frac{m^2_b}{M^2_W}\sqrt{s_a s_b} Y_2(r_H, r_H, s_a, s_b), \\ r_H &= \frac{M^2_{H^\pm}}{M^2_W}, \quad s_a = \frac{m^2_{ua}}{M^2_W}, \end{aligned}$$

where m_{ua} denotes the up-type quark mass of the a-th generation. The couplings proportional to the d-quark mass have been neglected. Since the values of $F^H_V(a;b)$ and $F^H_S(a;b)$ become dominantly large for $a = b = 3$, $L^H_{B^0_d}$ is approximately proportional to $(V^*_{31}V_{33})^2$. Except for large values of $\tan\beta$, F^H_S is negligible. The effective lagrangians $L^H_{B^0_s}$ and $L^H_{K^0}$ for B^0_s-$\bar{B}^0_s$ and K^0-$\bar{K}^0$ mixings are obtained

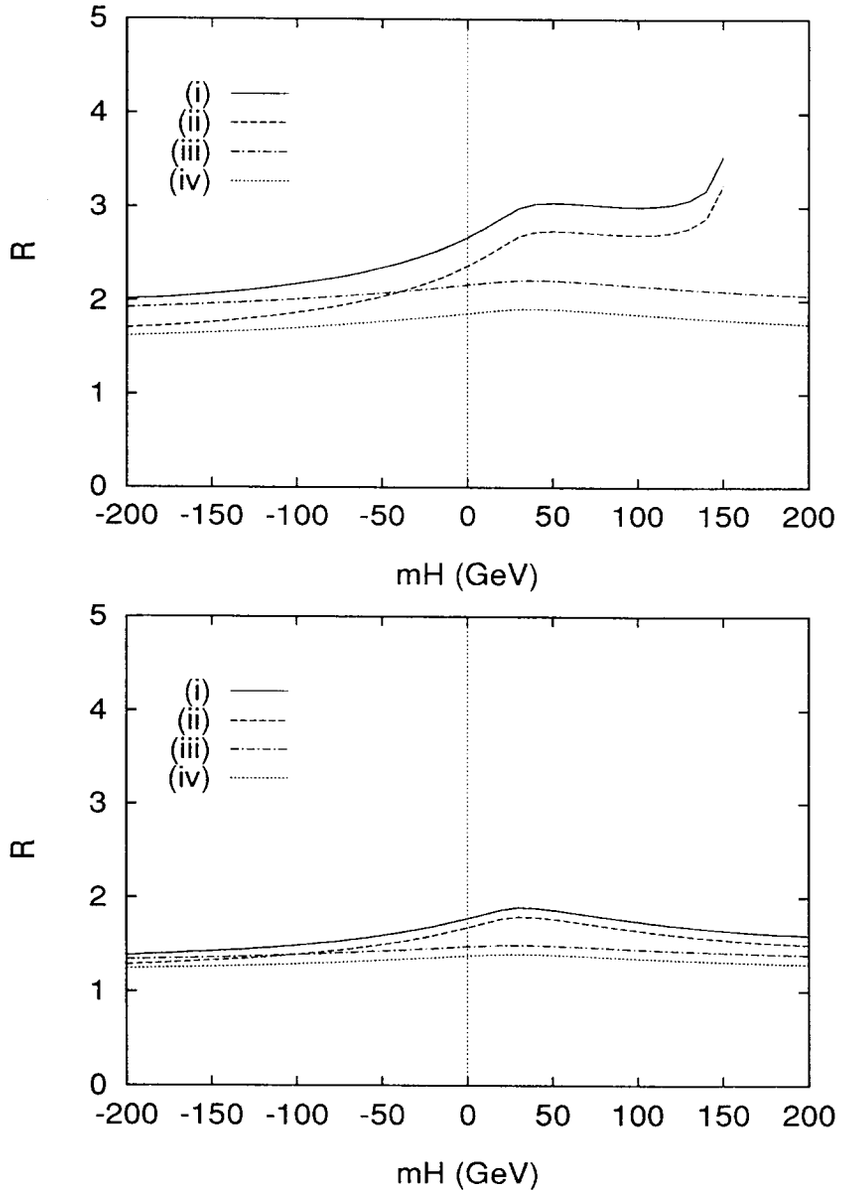

Figure 4: The ratio R for $\tilde{m}_2 = 200$ GeV: (Top) $\tan\beta = 1.2$, (Bottom) $\tan\beta = 2$. The values of $\tilde{m}_Q$ and $M_{H^\pm}$ for curves (i)–(iv) are given in table 3. The other parameters are set for $\tilde{m}_U = am_{3/2} = \tilde{m}_Q$ and $|c| = 0.3$.

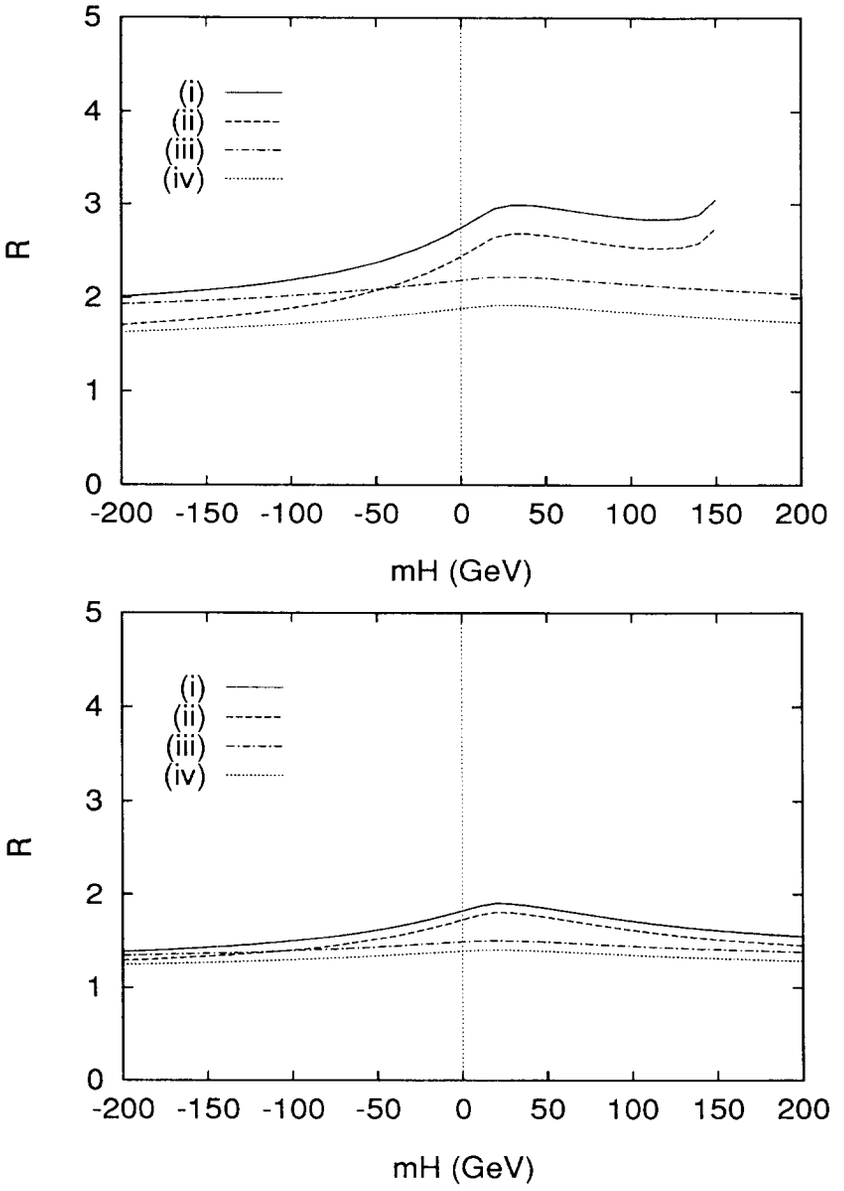

Figure 5: The ratio R for $\tilde{m}_2 = 300$ GeV. The other parameters are the same as in Fig. 4.

similarly. Approximately $L^H_{B^0_s}$ is proportional to $(V^*_{32}V_{33})^2$, while a priori $L^H_{K^0}$ has three terms proportional to $(V^*_{31}V_{32})^2$, $V^*_{31}V_{32}V^*_{21}V_{22}$, and $(V^*_{21}V_{22})^2$.

The standard W-boson interactions give, for B^0_d-$\bar{B}^0_d$ mixing, the effective lagrangian [12]

$$L^W_{B^0_d} = \frac{1}{8M^2_W}\left(\frac{g^2}{4\pi}\right)^2 \sum_{a,b} V^*_{a1}V_{a3}V^*_{b1}V_{b3} \\ F^W_V(a;b)\bar{d}\gamma^\mu\frac{1-\gamma_5}{2}b\bar{d}\gamma_\mu\frac{1-\gamma_5}{2}b, \tag{15}$$

$$F^W_V(a;b) = -\frac{1}{4}s_a s_b\{\frac{s^2_a-8s_a+4}{(s_a-s_b)(s_a-1)^2}\ln s_a + \frac{s^2_b-8s_b+4}{(s_b-s_a)(s_b-1)^2}\ln s_b \\ -\frac{3}{(s_a-1)(s_b-1)}\}.$$

The effective lagrangians $L^W_{B^0_s}$ and $L^W_{K^0}$ for B^0_s-$\bar{B}^0_s$ and K^0-$\bar{K}^0$ mixings are obtained similarly. Owing to a dominant value of $F^W_V(3;3)$, $L^W_{B^0_d}$ and $L^W_{B^0_s}$ are proportional to $(V^*_{31}V_{33})^2$ and $(V^*_{32}V_{33})^2$, respectively, while $L^W_{K^0}$ has three terms proportional to $(V^*_{31}V_{32})^2$, $V^*_{31}V_{32}V^*_{21}V_{22}$, and $(V^*_{21}V_{22})^2$.

We now discuss the SSM effects on two physical quantities, the mixing parameter x_d for B^0_d-$\bar{B}^0_d$ mixing and the CP violation parameter ϵ for K^0-$\bar{K}^0$ mixing [13]. The mixing parameter is defined by $x_d = \Delta M_{B_d}/\Gamma_{B_d}$, where ΔM_{B_d} and Γ_{B_d} denote the mass difference and the average width for the B^0_d-meson mass eigenstates. The mass difference is induced dominantly by the short distance contributions of box diagrams. We can express the mixing parameter as

$$x_d = \frac{G^2_F}{6\pi^2}M^2_W\frac{M_{B_d}}{\Gamma_{B_d}}f^2_{B_d}B_{B_d}|V^*_{31}V_{33}|^2\eta_{B_d}|F^W_V(3;3)+A^C_V+F^H_V(3;3)|, \tag{16}$$

where G_F, f_{B_d}, B_{B_d}, and η_{B_d} represent the Fermi constant, the B^0_d-meson decay constant, the bag factor for B^0_d-$\bar{B}^0_d$ mixing, and the QCD correction factor. We have neglected A^C_S and F^H_S. Assuming that QCD corrections for $F^W_V(3;3)$, A^C_V, and $F^H_V(3;3)$ do not differ much from each other, the same QCD factor has been multiplied. For K^0-$\bar{K}^0$ mixing, the mass difference ΔM_K receives large long distance contributions, which have not yet been calculated reliably. As a result, it is difficult to estimate short distance effects through ΔM_K. However, the CP violation parameter ϵ receives its dominant contribution from the short distance effects. This parameter can be written as

$$\epsilon = -e^{i\pi/4}\frac{G^2_F}{12\sqrt{2}\pi^2}M^2_W\frac{M_K}{\Delta M_K}f^2_K B_K$$

	(i)	(ii)	(iii)	(iv)
$\tilde{m}_Q$ (GeV)	200	200	300	300
$M_{H^\pm}$ (GeV)	100	200	100	200

Table 3: The values of $\tilde{m}_Q$ and $M_{H^\pm}$ for curves (i)–(iv) in Figs. 4 and 5.

$$\begin{aligned}
&\mathrm{Im}[(V_{31}^* V_{32})^2 \eta_{K33}(F_V^W(3;3) + A_V^C + F_V^H(3;3)) \\
&+(V_{21}^* V_{22})^2 \eta_{K22}(F_V^W(2;2) + F_V^H(2;2)) \\
&+2V_{31}^* V_{32} V_{21}^* V_{22} \eta_{K32}(F_V^W(3;2) + F_V^H(3;2))],
\end{aligned} \tag{17}$$

where f_K and B_K stand for the decay constant and the bag factor. The QCD correction factors are denoted by η_{Kab}.

The new contributions to x_d and ϵ in the SSM are A_V^C and F_V^H in eqs. (16) and (17). However, as long as $\tan\beta \gtrsim 1$, which is favored by the SSM, $F_V^H(2;2)$ and $F_V^H(3;2)$ are respectively much smaller than $F_V^W(2;2)$ and $F_V^W(3;2)$. Thus, the difference between the SSM and the SM contributions to ϵ is only in the term proportional to $(V_{31}^* V_{32})^2$. The effects of the SSM contributions to x_d and ϵ can be measured by the ratio

$$R = \frac{F_V^W(3;3) + A_V^C + F_V^H(3;3)}{F_V^W(3;3)}. \tag{18}$$

If there exists no sizable new contribution, R approaches one.

In Fig. 4 we show R as a function of the higgsino mass parameter m_H, taking $\tilde{m}_2 = 200$ GeV, $\tilde{m}_Q = 200$, 300 GeV, $M_{H^\pm} = 100$, 200 GeV, and $\tan\beta = 1.2$, 2. Curves (i)–(iv) correspond to four sets of values for $\tilde{m}_Q$ and $M_{H^\pm}$ listed in table 3. The values of the other SSM parameters are set for $\tilde{m}_U = am_{3/2} = \tilde{m}_Q$ and $|c| = 0.3$. In Fig. 5 the ratio R is shown taking $\tilde{m}_2 = 300$ GeV and the same values as in Fig. 4 for the other parameters. The lighter t-squark and the lighter chargino masses corresponding to these parameter values can been seen in Figs. 2 and 3, respectively. The chargino, charged Higgs boson, and W-boson contributions have the same sign and interfere constructively. The ratio R is around 2 or larger for $\tan\beta = 1.2$, while it becomes smaller for $\tan\beta = 2$. This dependence on $\tan\beta$ arises from the Yukawa coupling constants in the chargino and the charged Higgs boson interactions as seen in eqs. (12) and (14). Both the values of $\tilde{m}_Q$ and $M_{H^\pm}$ also affect R significantly. For $\tilde{m}_Q = 200$ GeV and $\tan\beta = 1.2$, R can be enhanced up to $R \sim 3$, owing to a small value for the lighter t-squark mass. The ratio R does not vary much with $\tilde{m}_2$.

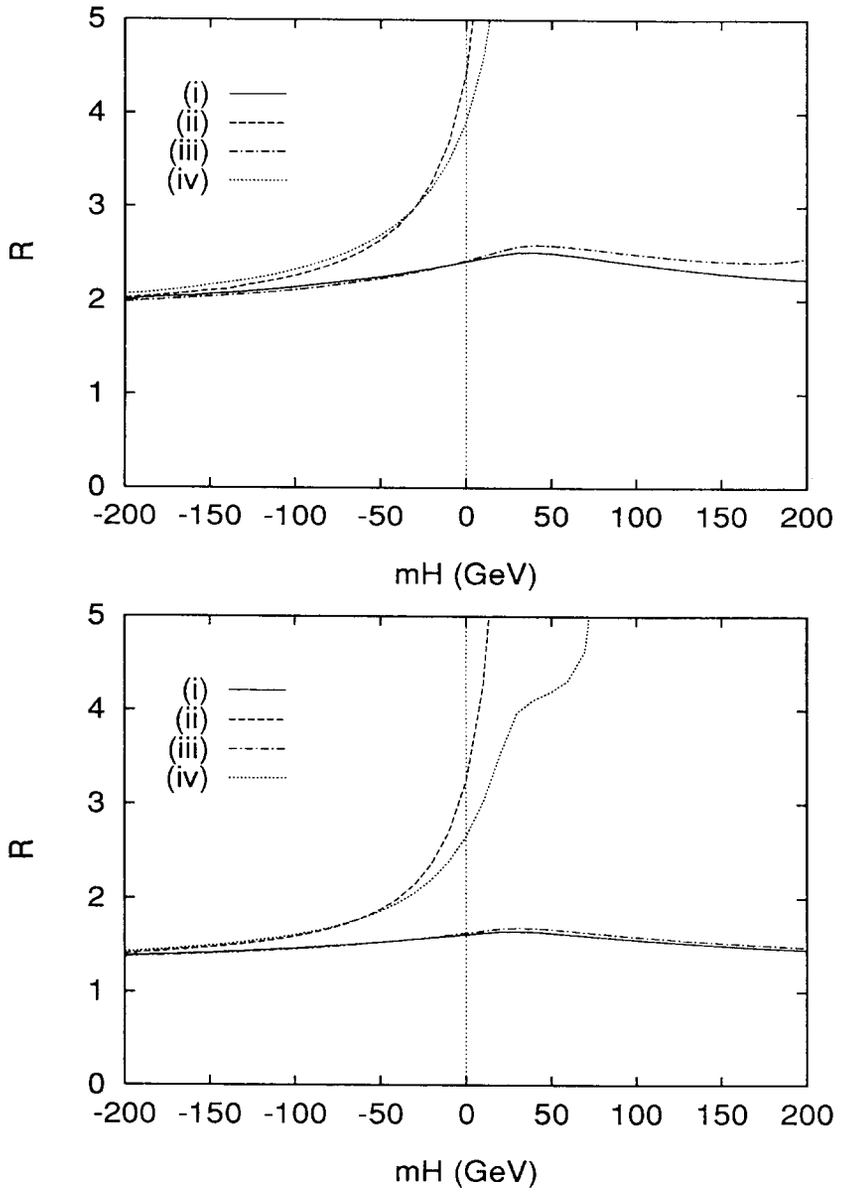

Figure 6: The ratio R: (Top) $\tan\beta = 1.2$, (Bottom) $\tan\beta = 2$. The values of $am_{3/2}/\tilde{m}_Q$ and $|c|$ for curves (i)–(iv) are given in table 4. The other parameters are set for $\tilde{m}_2 = 200$ GeV, $M_{H^\pm} = 100$ GeV, and $\tilde{m}_Q = \tilde{m}_U = 200$ GeV.

	(i)	(ii)	(iii)	(iv)
$am_{3/2}/\tilde{m}_Q$	0.5	1.5	1.0	1.0
$\|c\|$	0.3	0.3	0.1	0.6

Table 4: The values of $am_{3/2}/\tilde{m}_Q$ and $|c|$ for curves (i)–(iv) in Fig. 6.

The a- and c-dependences of R can be seen in Fig. 6, where we take four sets of values for $am_{3/2}/\tilde{m}_Q$ and $|c|$ listed in table 4, and $\tan\beta = 1.2$, 2. The other parameter values are set for $\tilde{m}_2 = 200$ GeV, $M_{H^\pm} = 100$ GeV, and $\tilde{m}_Q = \tilde{m}_U = 200$ GeV. The parameters a and c affect the masses of the t-squarks through eq. (7). As $|a|$ or $|c|$ increases, the lighter t-squark mass becomes smaller, leading to a larger value for R.

Summarizing these results, the SSM contribution can be enhanced to be $R \sim 2$, if $\tan\beta \sim 1$ and $\tilde{m}_{\omega 1}, \tilde{M}_{t1}, M_{H^\pm} \sim 100$ GeV. The ratio R could even be larger for smaller values of $\tilde{m}_{\omega 1}$ and $\tilde{M}_{t1}$. Within the SSM parameter space bounded by presently available experiments, for sizable regions the SSM contribution is predicted to be different from the SM contribution by of order unity. The value of R is not so enhanced for $\tan\beta \gtrsim 2$ unless $\tilde{m}_{\omega 1}$ and $\tilde{M}_{t1}$ are very small. However, if $\tan\beta$ is much larger than 10, A_S^C in eq. (11) for B_d^0-$\bar{B}_d^0$ mixing becomes nonnegligible. It is then necessary to take into consideration the effect of the quark operator proportional to A_S^C. In this case, a sizable new SSM contribution to B_d^0-$\bar{B}_d^0$ mixing may be yielded through this quark operator.

4 Constraints and predictions

In this section we analyze the implications of an enhancement of R for the determination of the CKM parameters and discuss the predictions for CP asymmetries in B^0-meson decays and for the mixing parameter x_s of B_s^0-$\bar{B}_s^0$ mixing. We use the standard parametrization of the CKM matrix:

$$V = \begin{pmatrix} c_{12}c_{13} & s_{12}c_{13} & s_{13}e^{-i\delta} \\ -s_{12}c_{23} - c_{12}s_{23}s_{13}e^{i\delta} & c_{12}c_{23} - s_{12}s_{23}s_{13}e^{i\delta} & s_{23}c_{13} \\ s_{12}s_{23} - c_{12}c_{23}s_{13}e^{i\delta} & -c_{12}s_{23} - s_{12}c_{23}s_{13}e^{i\delta} & c_{23}c_{13} \end{pmatrix}, \qquad (19)$$

where $c_{ab} = \cos\theta_{ab}$ and $s_{ab} = \sin\theta_{ab}$. Without loss of generality, the angles θ_{12}, θ_{23}, and θ_{13} can be taken to lie in the first quadrant: $\sin\theta_{ab} > 0$, $\cos\theta_{ab} > 0$. At present and within the framework of the SM, experiments give [3, 14]: $|V_{12}| \equiv$

$|V_{us}| = 0.2205 \pm 0.0018$, $|V_{23}| \equiv |V_{cb}| = 0.04 \pm 0.004$, and $|V_{13}/V_{23}| \equiv |V_{ub}/V_{cb}| = 0.08 \pm 0.02$. Since these values have been measured through the processes for which new contributions by the SSM, if any, are negligible, they are also valid in the SSM. The three mixing angles θ_{ab} are readily determined from the above experimental input: $\sin\theta_{12} = |V_{12}|$, $\sin\theta_{23} = |V_{23}|$, and $\sin\theta_{13} = |V_{13}|$, where we have taken into account the smallness of $\sin\theta_{13}$ to put $\cos\theta_{13} = 1$, to an excellent accuracy. The only remaining undetermined CKM parameter is the CP-violating phase δ, which can be measured by the mixing parameter x_d or the CP violation parameter ϵ, through eq. (16) or (17). The experimental measurements of x_d and ϵ have already been achieved fairly precisely as $x_d = 0.71 \pm 0.06$ and $|\epsilon| = 2.26 \times 10^{-3}$ [3]. Therefore, for $R > 1$, the SSM and the SM predict different values for δ.

The value of δ is determined as a function of R independently by x_d and ϵ. Imposing consistency of these two evaluations, one can obtain the values of δ and R. However, one has to take into account large theoretical uncertainties in f_{B_d}, B_{B_d}, and B_K, which do not depend on whether the underlying model is the SM or the SSM. We assume, for definiteness, a recent result of lattice calculation 180 MeV $< f_{B_d}\sqrt{B_{B_d}} <$ 260 MeV [15] and a combined result of lattice [16] and 1/N [17] calculations $0.6 < B_K < 0.9$.

We show the range of the ratio R derived from the experimental values of x_d and ϵ as a function of $\cos\delta$ in Figs. 7, 8, and 9 for $|V_{13}/V_{23}| = 0.06$, 0.08, and 0.1, respectively. For each value of $|V_{13}/V_{23}|$ we take $|V_{23}| = 0.036$, 0.04, and 0.044. The sign of $\sin\delta$ is positive in order to correctly give ϵ. The value of x_d is fixed at its experimental central value $x_d = 0.71$. For the QCD correction factors we have used $\eta_{B_d} = 0.55$ in eq. (16) and $\eta_{K33} = 0.57$, $\eta_{K22} = 1.1$, and $\eta_{K32} = 0.36$ in eq. (17) [18]. The region between the solid curves and that between the dashed curves are respectively allowed by x_d and ϵ. The upper curves correspond to lower limits for $f_{B_d}\sqrt{B_{B_d}}$ and B_K, and the lower curves to upper limits. The overlappling region is the consistently allowed region. Note that $R \geq 1$ for the SSM and $R = 1$ for the SM. Obviously, the allowed region for the SM is always contained in that for the SSM. If there are some new contributions to B_d^0-$\bar{B}_d^0$ and K^0-$\bar{K}^0$ mixings similar to those of the SSM but with different sign, the allowed region with $R < 1$ has also to be taken into consideration.

In case of $|V_{13}/V_{23}| = 0.06$ the allowed region exists only for a larger value of $|V_{23}|$. The values of R and $\cos\delta$ are constrained as $0.7 \lesssim R \lesssim 1.4$, $-0.4 \lesssim \cos\delta \lesssim 0.7$, and there is not much room for new contributions to B_d^0-$\bar{B}_d^0$ and K^0-$\bar{K}^0$ mixings.

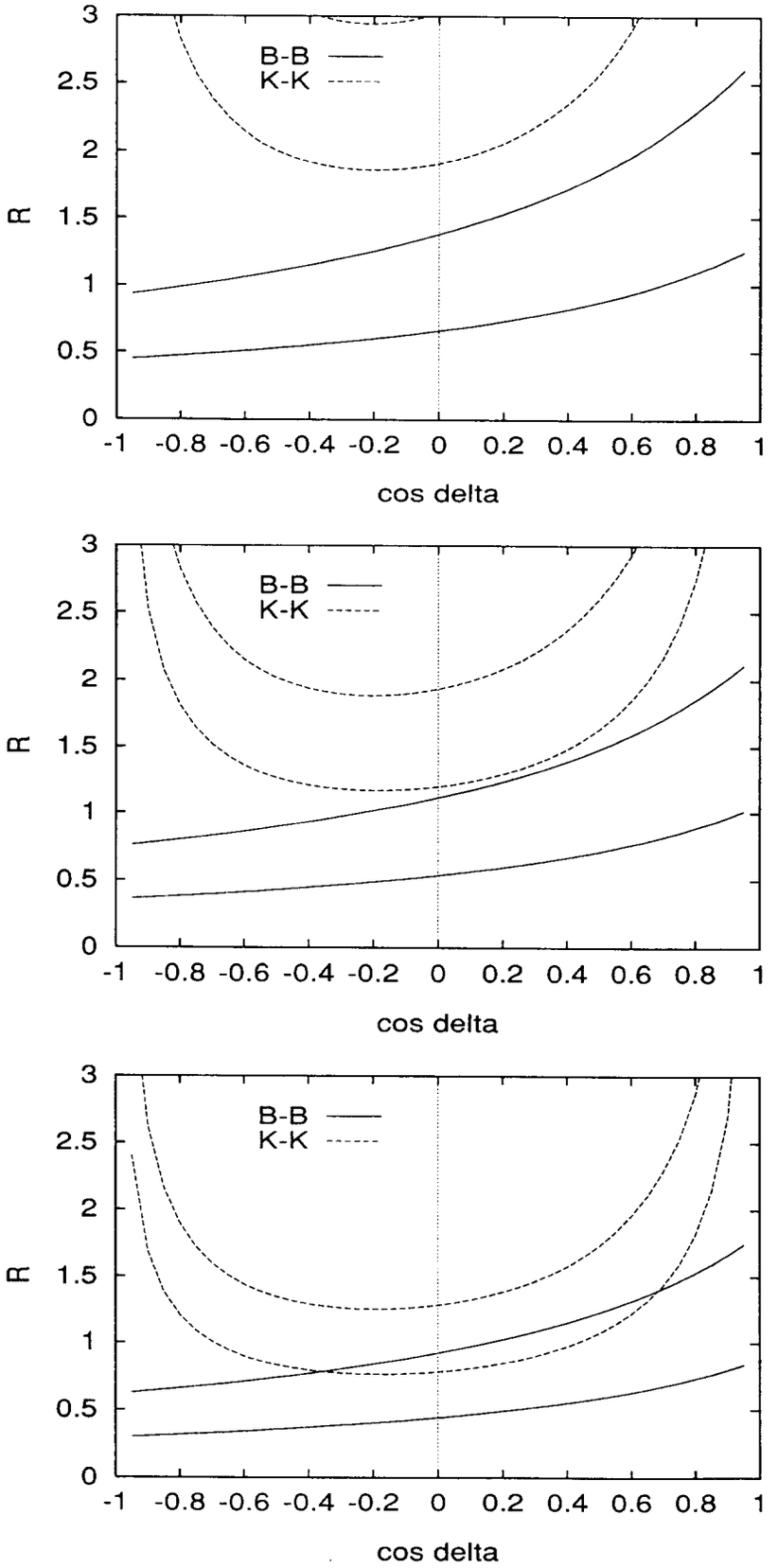

Figure 7: The ratio R allowed by the experimental values of x_d and ϵ for $|V_{13}/V_{23}| = 0.06$: (Top) $|V_{23}| = 0.036$, (Middle) $|V_{23}| = 0.04$, (Bottom) $|V_{23}| = 0.044$.

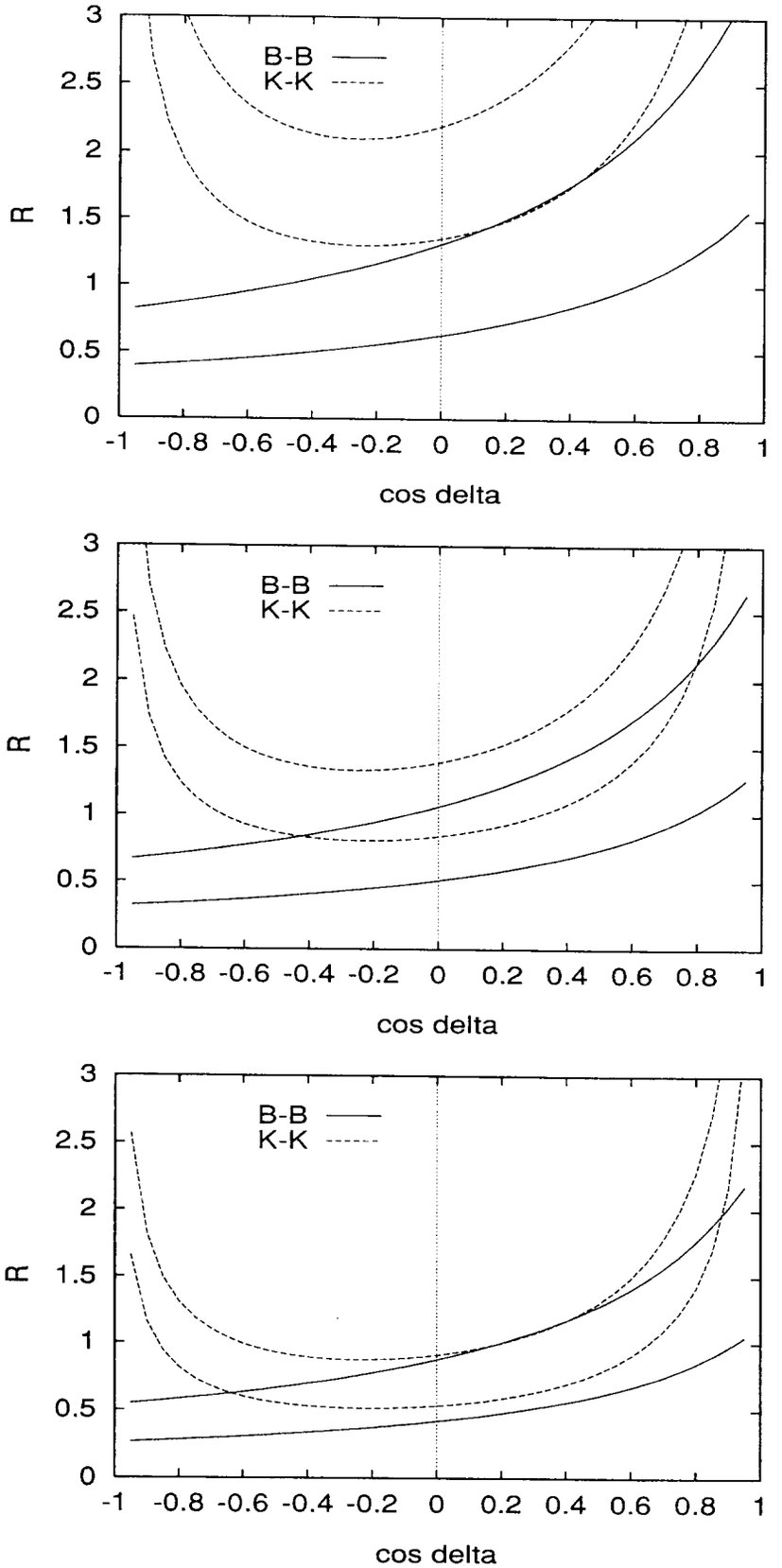

Figure 8: The ratio R allowed by the experimental values of x_d and ϵ for $|V_{13}/V_{23}| = 0.08$: (Top) $|V_{23}| = 0.036$, (Middle) $|V_{23}| = 0.04$, (Bottom) $|V_{23}| = 0.044$.

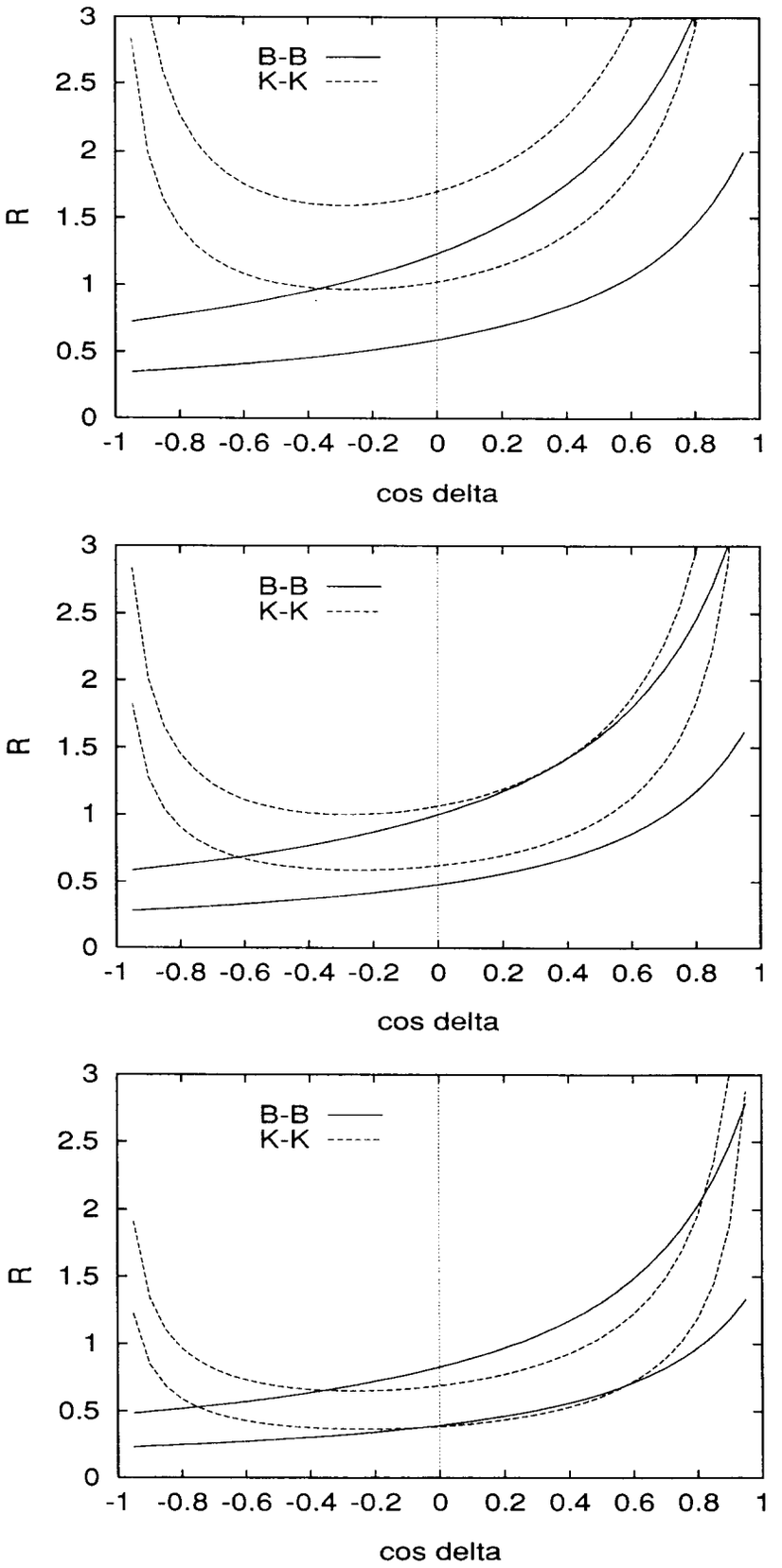

Figure 9: The ratio R allowed by the experimental values of x_d and ϵ for $|V_{13}/V_{23}| = 0.1$: (Top) $|V_{23}| = 0.036$, (Middle) $|V_{23}| = 0.04$, (Bottom) $|V_{23}| = 0.044$.

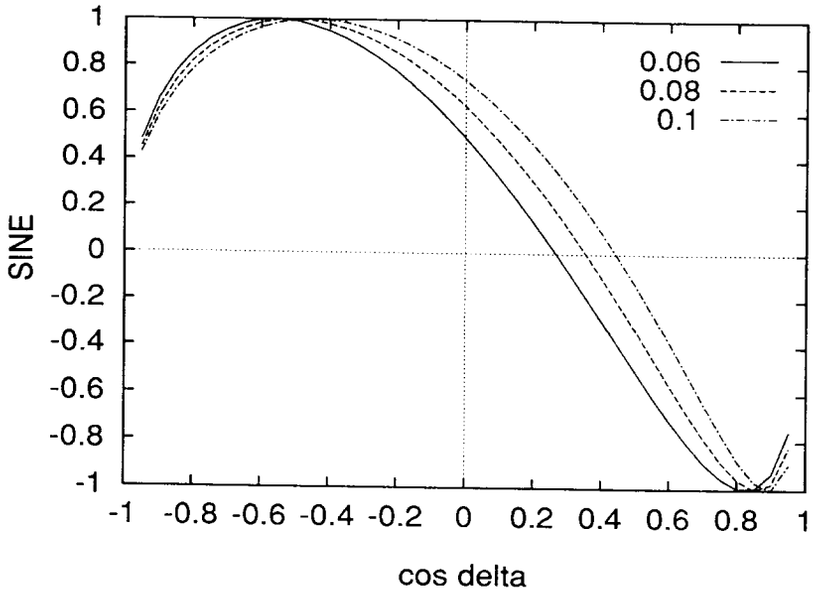

Figure 10: The value of $\sin 2\phi_\alpha$ for the three values of $|V_{13}/V_{23}|$.

For $|V_{13}/V_{23}| = 0.06$ and $|V_{23}| \lesssim 0.04$, neither the SM nor the SSM can consistently accommodate x_d and ϵ. As the value of $|V_{13}/V_{23}|$ increases, a wider region becomes allowed. The values of R and $\cos\delta$ are $0.5 \lesssim R \lesssim 2.2$, $-0.7 \lesssim \cos\delta \lesssim 0.9$ and $0.3 \lesssim R \lesssim 3.2$, $-0.8 \lesssim \cos\delta \lesssim 0.9$ for $|V_{13}/V_{23}| = 0.08$ and 0.1, respectively, although these ranges can be narrower for a specific value of $|V_{23}|$. In case of $|V_{23}| = 0.036$ there is almost no allowed region for $|V_{13}/V_{23}| \lesssim 0.08$, and the allowed region for a larger value of $|V_{13}/V_{23}|$ is mostly inconsistent with the SM. If we assume the central values $|V_{13}/V_{23}| = 0.08$ and $|V_{23}|$=0.04, the allowed ranges are $0.8 \lesssim R \lesssim 2.1$ and $-0.5 \lesssim \cos\delta \lesssim 0.8$, while $-0.1 \lesssim \cos\delta \lesssim 0.3$ for the SM, which corresponds to $R = 1$.

The above analysis, taking into account the present theoretical and experimental knowledge on x_d, ϵ, $|V_{13}/V_{23}|$, $|V_{23}|$, and $|V_{12}|$, gives the constraints $0.3 \lesssim R \lesssim 3.2$ and $-0.8 \lesssim \cos\delta \lesssim 0.9$. Consequently, the SSM parameter regions for $R > 3$ are mostly ruled out, which makes the existence of a very light t-squark unlikely [19]. More precise determinations of $|V_{13}/V_{23}|$ and $|V_{23}|$ expected in the near future can further constrain R and $\cos\delta$. If $|V_{13}/V_{23}| < 0.08$ and $|V_{23}| < 0.04$ are found, the constraints become very tight in both the SSM and the SM. For larger values of $|V_{13}/V_{23}|$ and $|V_{23}|$, there are wider ranges of R and $\cos\delta$ which are allowed. These ranges will become narrower, if $f_{B_d}\sqrt{B_{B_d}}$ and B_K are determined more precisely, whereas uncertainties in the experimental measurements of x_d and m_t are already

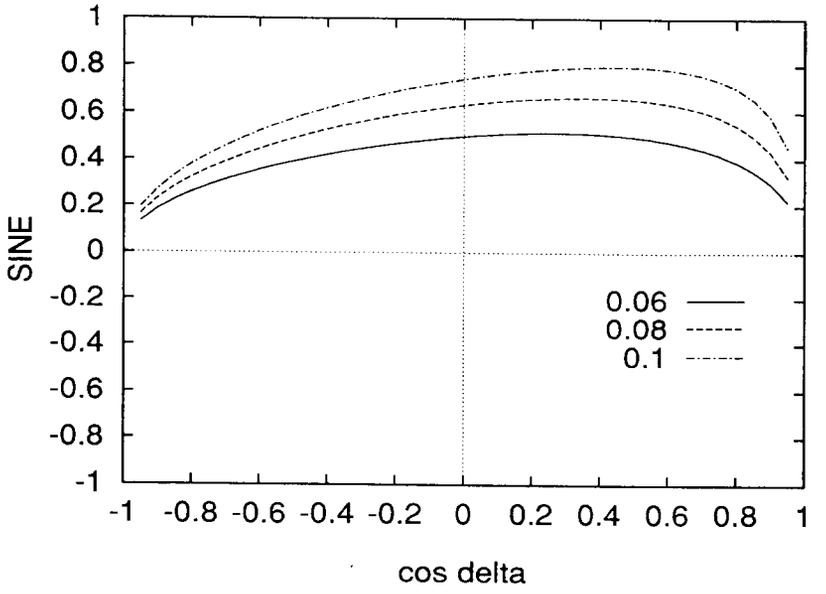

Figure 11: The value of $\sin 2\phi_\beta$ for the three values of $|V_{13}/V_{23}|$.

not so severe.

We now consider CP asymmetries in B^0-meson decays. Since the CKM phase δ is the only source of CP violation, CP asymmetries crucially depend on δ. Once $\cos\delta$ is determined, the allowed values of the asymmetries can be derived. Conversely, the measurement of the asymmetries will constrain the allowed values of $\cos\delta$ and R.

The CP asymmetries enable to measure the angles of the unitarity triangle, which are simply related to the arguments of rephasing invariant quartets by[§]

$$\begin{aligned} \phi_\alpha &= \arg(-V_{31}V_{33}^*V_{11}^*V_{13}), \quad \phi_\beta = \arg(-V_{21}V_{23}^*V_{31}^*V_{33}), \\ \phi_\gamma &= \arg(-V_{11}V_{13}^*V_{21}^*V_{23}). \end{aligned} \tag{20}$$

For instance, the decays $B_d^0 \to \pi^+\pi^-$, $B_d^0 \to \psi K_S$, and $B_s^0 \to \rho K_S$ could determine $\sin 2\phi_\alpha$, $\sin 2\phi_\beta$, and $\sin 2\phi_\gamma$, respectively. From eqs. (19) and (20), these asymmetries can be expressed in terms of $\cos\delta$ and $r \equiv \cot\theta_{12}(\sin\theta_{13}/\sin\theta_{23})$, to an excellent accuracy:

$$\begin{aligned} \sin 2\phi_\alpha &= \frac{2\sin\delta(r-\cos\delta)}{1-2r\cos\delta+r^2}, \quad \sin 2\phi_\beta = \frac{2r\sin\delta(1-r\cos\delta)}{1-2r\cos\delta+r^2}, \\ \sin 2\phi_\gamma &= \sin 2\delta. \end{aligned} \tag{21}$$

[§]The angles ϕ_α, ϕ_β, and ϕ_γ defined here are equivalent to the angles usually denoted by α, β, and γ, respectively, in the literature.

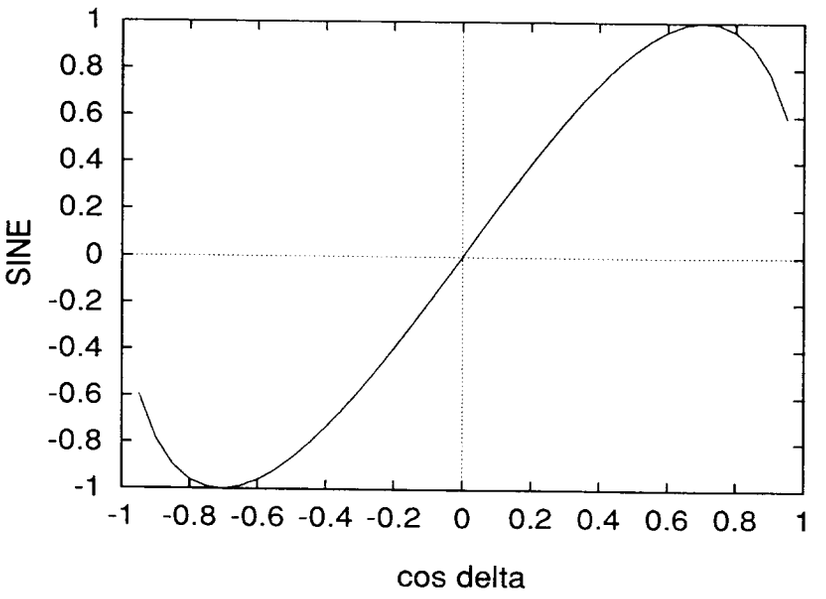

Figure 12: The value of $\sin 2\phi_\gamma$.

The values of $\sin 2\phi_\alpha$ and $\sin 2\phi_\beta$ only depend on $\cos\delta$ and r, while $\phi_\gamma = \delta$. In Figs. 10 and 11, we plot the values of $\sin 2\phi_\alpha$ and $\sin 2\phi_\beta$, as a function of $\cos\delta$, for $|V_{13}/V_{23}| = 0.06$, 0.08, 0.1. In Fig. 12, we plot the value of $\sin 2\phi_\gamma$. In most of the plausible ranges for $\cos\delta$ inferred from Figs. 7–9, $\sin 2\phi_\alpha$ and $\sin 2\phi_\gamma$ monotonously change between -1 and 1, while $\sin 2\phi_\beta$ does not vary much with $\cos\delta$. The dependence on $|V_{13}/V_{23}|$ is weak for both $\sin 2\phi_\alpha$ and $\sin 2\phi_\beta$. These show the reasons why, in the SM, the prediction of $\sin 2\phi_\beta$ has been made more specifically than those of $\sin 2\phi_\alpha$ and $\sin 2\phi_\gamma$ [20]. Taking into account the present constraints on $\cos\delta$ and $|V_{13}/V_{23}|$, the value of $\sin 2\phi_\beta$ should satisfy $0.4 \lesssim \sin 2\phi_\beta \lesssim 0.8$, whereas $\sin 2\phi_\alpha$ and $\sin 2\phi_\gamma$ can have any values from -1 to 1.

The mixing parameter x_s for B_s^0-$\bar{B}_s^0$ mixing is given by an expression entirely analogous to eq. (16). Of special importance is the ratio of x_s to x_d, which, neglecting $\mathrm{SU}(3)_{flavor}$ breaking, is given by

$$\frac{x_s}{x_d} = \frac{|V_{32}|^2}{|V_{31}|^2}. \tag{22}$$

From eqs. (19) and (22), one can obtain, to an excellent accuracy:

$$\frac{x_s}{x_d} = \frac{\cot^2\theta_{12} + 2r\cos\delta}{1 - 2r\cos\delta + r^2}. \tag{23}$$

In Fig. 13 the ratio x_s/x_d is depicted as a function of $\cos\delta$ for $|V_{13}/V_{23}| = 0.06$, 0.08, 0.1. As $\cos\delta$ increases, x_s/x_d monotonously increases. The present constraints on

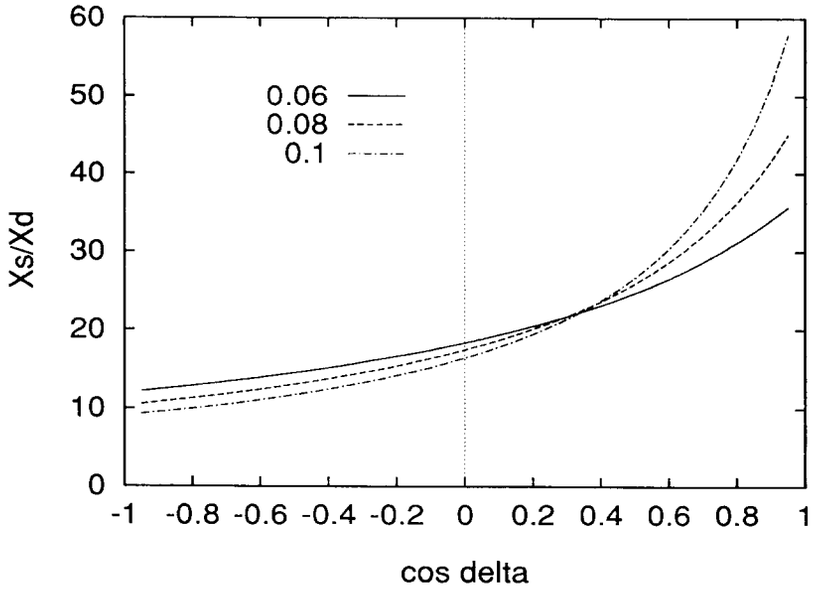

Figure 13: The ratio of x_s to x_d for the three values of $|V_{13}/V_{23}|$.

$\cos\delta$ and $|V_{13}/V_{23}|$ give $10 \lesssim x_s/x_d \lesssim 56$. It is worth emphasizing that the three CP asymmetries as well as the ratio x_s/x_d only depend on $\cos\delta$ and $|V_{13}/V_{23}|$.

From Figs. 7–9, it is clear that the value of $\cos\delta$ in the SSM can be larger than what is allowed by the SM. For instance, if $|V_{13}/V_{23}| = 0.08$ and $|V_{23}| = 0.04$, the range $0.3 \lesssim \cos\delta \lesssim 0.8$ is allowed only in the SSM. Therefore, $\sin 2\phi_i$ $(i = \alpha, \beta, \gamma)$ and x_s/x_d could have values outside the ranges predicted by the SM. In table 5 we give the predicted values of $\sin 2\phi_i$ and x_s/x_d in the SSM and in the SM for $(|V_{13}/V_{23}|, |V_{23}|) = (0.08, 0.04)$ (a), (0.08, 0.044) (b), (0.1, 0.04) (c) corresponding to Figs. 8 (Middle), 8 (Bottom), 9 (Middle), respectively. In each case there are wide ranges of $\sin 2\phi_\alpha$, $\sin 2\phi_\gamma$, and/or x_s/x_d which are possible only in the SSM. If the experimental values are found in these ranges, then this would indicate that $R > 1$, with significant new contributions to B^0-$\bar{B}^0$ and K^0-$\bar{K}^0$ mixings arising from the SSM. For case (a), which corresponds to the experimental central values for $|V_{13}/V_{23}|$ and $|V_{23}|$, the possible experimental results $\sin 2\phi_\alpha < 0$, $\sin 2\phi_\gamma \sim 1$, and $x_s/x_d \sim 30$ suggest the SSM effects.

The measurements of $\sin 2\phi_i$ and x_s/x_d can give further information. Since $\sin 2\phi_\alpha$, $\sin 2\phi_\gamma$, and x_s/x_d sensitively reflect the value of $\cos\delta$, they could be used to precisely determine $\cos\delta$. On the other hand, $\sin 2\phi_\beta$ is insensitive to the value of $\cos\delta$, but it could be used to determine $|V_{13}/V_{23}|$. In order to illustrate the various possibilities, we consider the case that the experiments give $\sin 2\phi_\alpha = -0.5 \pm 0.1$

(a)

	SSM	SM
$\sin 2\phi_\alpha$	$(-0.96, 0.74)$	$(0.15, 0.74)$
$\sin 2\phi_\beta$	$(0.55, 0.66)$	$(0.61, 0.66)$
$\sin 2\phi_\gamma$	$(-0.18, 1.00)$	$(-0.18, 0.54)$
x_s/x_d	$(17, 36)$	$(17, 21)$

(b)

	SSM	SM
$\sin 2\phi_\alpha$	$(-1.00, 0.31)$	$(-0.65, 0.31)$
$\sin 2\phi_\beta$	$(0.46, 0.66)$	$(0.63, 0.66)$
$\sin 2\phi_\gamma$	$(0.39, 1.00)$	$(0.39, 0.98)$
x_s/x_d	$(20, 40)$	$(20, 30)$

(c)

	SSM	SM
$\sin 2\phi_\alpha$	$(-1.00, 0.73)$	$(-0.15, 0.73)$
$\sin 2\phi_\beta$	$(0.56, 0.80)$	$(0.74, 0.80)$
$\sin 2\phi_\gamma$	$(0.02, 1.00)$	$(0.02, 0.88)$
x_s/x_d	$(17, 53)$	$(17, 27)$

Table 5: The ranges of $\sin 2\phi_\alpha$, $\sin 2\phi_\beta$, $\sin 2\phi_\gamma$, and x_s/x_d predicted by the SSM and the SM: (a) $|V_{13}/V_{23}| = 0.08$, $|V_{23}| = 0.04$, (b) $|V_{13}/V_{23}| = 0.08$, $|V_{23}| = 0.044$, (c) $|V_{13}/V_{23}| = 0.1$, $|V_{23}| = 0.04$.

(a)

$\lvert V_{13}/V_{23}\rvert$	0.07	0.08	0.09
$\cos\delta$	$(0.50, 0.58)$	$(0.54, 0.61)$	$(0.58, 0.65)$
$\sin 2\phi_\beta$	$(0.56, 0.58)$	$(0.64, 0.65)$	$(0.70, 0.72)$
$\sin 2\phi_\gamma$	$(0.87, 0.95)$	$(0.91, 0.97)$	$(0.95, 0.99)$
x_s/x_d	$(25, 27)$	$(27, 29)$	$(29, 32)$
R	$(1.1, 1.7)$	$(1.0, 1.9)$	$(0.9, 2.1)$

(b)

$\lvert V_{13}/V_{23}\rvert$	0.07	0.08	0.09
$\cos\delta$	$(-0.02, 0.10)$	$(0.03, 0.14)$	$(0.07, 0.19)$
$\sin 2\phi_\beta$	$(0.56, 0.58)$	$(0.64, 0.65)$	$(0.70, 0.72)$
$\sin 2\phi_\gamma$	$(-0.04, 0.20)$	$(0.06, 0.28)$	$(0.14, 0.37)$
x_s/x_d	$(18, 19)$	$(18, 19)$	$(18, 20)$
R	$(0.8, 1.3)$	$(0.6, 1.3)$	$(0.6, 1.3)$

Table 6: The ranges of $\cos\delta$, $\sin 2\phi_\beta$, $\sin 2\phi_\gamma$, x_s/x_d, and R predicted by the measurement of $\sin 2\phi_\alpha$ for $|V_{13}/V_{23}| = 0.07, 0.08, 0.09$: (a) $\sin 2\phi_\alpha = -0.5 \pm 0.1$, (b) $\sin 2\phi_\alpha = 0.5 \pm 0.1$. The range for R is derived under the assumption of $|V_{23}| = 0.04 \pm 0.002$.

(a), 0.5 ± 0.1 (b). The measurement of $\sin 2\phi_\alpha$ determines the value of $\cos\delta$, which then predicts the values of $\sin 2\phi_\beta$, $\sin 2\phi_\gamma$, and x_s/x_d, as given in table 6 for $|V_{13}/V_{23}| = 0.07, 0.08, 0.09$. Also given is the predicted range of R, assuming $|V_{23}| = 0.04 \pm 0.002$. Even if there is an uncertainty in $|V_{13}/V_{23}|$ of 0.08 ± 0.01, the possible value of $\cos\delta$ is restricted within $0.5 - 0.7$ in case (a) and $0.0 - 0.2$ in case (b). Moreover, the difference of 0.01 for $|V_{13}/V_{23}|$ leads to a sizable difference in the value of $\sin 2\phi_\beta$, which may be detectable. If $\sin 2\phi_\beta$ is measured with sufficient accuracy, the value of $|V_{13}/V_{23}|$ can be determined. As the values of $\cos\delta$, $|V_{13}/V_{23}|$, and $|V_{23}|$ are determined more precisely, the bounds on R are tightened. In case (a), if $0.07 \leq |V_{13}/V_{23}| \leq 0.08$ and $0.038 \leq |V_{23}| \leq 0.042$ hold, $1.0 \lesssim R \lesssim 1.9$ is predicted, suggesting the existence of SSM effects on B^0-$\bar{B}^0$ and K^0-$\bar{K}^0$ mixings.

Finally we comment on how future improvements of the theoretical calculations for $f_{B_d}\sqrt{B_{B_d}}$ and B_K affect our analyses. As seen in Figs. $7-9$, the allowed regions are bounded by the curves for $f_{B_d}\sqrt{B_{B_d}} = 180$ MeV and $B_K = 0.9$ in wide ranges of $|V_{13}/V_{23}|$ and $|V_{23}|$. Therefore, if the lower limit of $f_{B_D}\sqrt{B_{B_d}}$ increases, or if the

upper limit of B_K decreases, the allowed regions become more restricted, making the predictions more definitive. The small changes of the upper limit of $f_{B_d}\sqrt{B_{B_d}}$ and the lower limit of B_K essentially do not affect the results of this paper.

5 Conclusions

In the SSM, B^0-$\bar{B}^0$ and K^0-$\bar{K}^0$ mixings receive contributions from box diagrams in which charginos and up-type squarks, or charged Higgs bosons and up-type quarks are exchanged. We have calculated the ratio R of the total SSM contribution to x_d to the contribution in the SM. The new SSM contributions interfere constructively with the standard W-boson contributions and the ratio R can be significantly different from unity, contrary to earlier expectations. If $\tan\beta$ has a value around unity and a chargino, a t-squark, and/or a charged Higgs boson are not much heavier than 100 GeV, the SSM contribution becomes about twice as large as the SM contribution. Recently, it has been suggested [21] that these parameter values could also lead to sizable vertex corrections to the $Zb\bar{b}$ vertex in the SSM, which might explain the reported discrepancy in $\Gamma(Z \to b\bar{b})$ between the experiments and the SM.

The enhancement of the contributions to B^0-$\bar{B}^0$ and K^0-$\bar{K}^0$ mixings leads to a SSM value for the CP-violating phase δ of the CKM matrix which is different from that obtained within the SM, for the same experimental values of the mixing parameter x_d and the CP violation parameter ϵ. We have determined the ranges of $\cos\delta$ and R allowed by x_d and ϵ. The present uncertainties in $|V_{13}/V_{23}|$, $|V_{23}|$, $f_{B_d}\sqrt{B_{B_d}}$, and B_K are still large, and the derived ranges for $\cos\delta$ and R vary with the values of those quantities. It would be premature to draw a definitive prediction. However, there is not much room for $R > 3$, so that certain SSM parameter regions which predict a light t-squark are excluded. If the present experimental central values for $|V_{13}/V_{23}|$ and $|V_{23}|$ are in the vicinities of the actual values, $\cos\delta$ and R should respectively lie in the ranges $-0.1-0.8$ and $1.0-2.1$, for the SSM, while $-0.1 \lesssim \cos\delta \lesssim 0.3$ should hold for the SM, where $R = 1$. Note that large ambiguity for the determination of $\cos\delta$ and R stems from the uncertainties in $f_{B_d}\sqrt{B_{B_d}}$ and B_K. Therefore, it is important to improve theoretical calculations for $f_{B_d}\sqrt{B_{B_d}}$ and B_K as well as experimental measurements for the CKM matrix.

The CP-violating phase δ can also be probed by CP asymmetries in B^0-meson decays and B_s^0-$\bar{B}_s^0$ mixing, which will be studied experimentally in the near future.

We have shown the possibility that the precise measurements of $\sin 2\phi_\alpha$, $\sin 2\phi_\beta$, $\sin 2\phi_\gamma$, and x_s/x_d disclose values of $\cos\delta$ and R which are not allowed in the SM, thus providing indirect evidence for the SSM. Even if only $\sin 2\phi_\alpha$ and $\sin 2\phi_\beta$ are measured, the values of $\cos\delta$ and R could be well determined. At B-factories, the measurements of $\sin 2\phi_\alpha$ and $\sin 2\phi_\beta$ are expected to be performed fairly precisely, and the values of $|V_{13}/V_{23}|$ and $|V_{23}|$ will be known with greater accuracy. The evaluations of $\cos\delta$ and R will provide a good tool to examine the SSM.

The SSM interactions mediated by the charginos and the charged Higgs bosons in eqs. (9) and (10) could also sizably contribute to the radiative quark decays $b \to s\gamma$ and $b \to d\gamma$, which are observed as radiative B-meson decays. In particular, the chargino contributions are enhanced in the SSM parameter regions with $\tan\beta \gtrsim 10$ [8, 22], where the new SSM contributions to B^0-$\bar{B}^0$ and K^0-$\bar{K}^0$ mixings are small. In addition, the ratio $\Gamma(b \to s\gamma)/\Gamma(b \to d\gamma)$ is given by the same equation as x_s/x_d in eq. (22). Radiative B-meson decays will therefore provide information on the SSM which is complimentary to that given by B^0-$\bar{B}^0$ mixings.

The masses of the supersymmetric particles which could lead to sizable new SSM contributions to B^0-$\bar{B}^0$ and K^0-$\bar{K}^0$ mixings lie within reach of the next high energy collider experiments, such as LEP II and Next Linear Colliders. If, in the future, more accurate values for $|V_{13}/V_{23}|$ and $|V_{23}|$ together with the measurement of CP asymmetries in B^0-meson decays and x_s/x_d indicate that a consistent fitting can only be obtained for $R > 1$, there is a good possibility that supersymmetric particles be found in those high energy experiments. On the other hand, if a consistent fitting is obtained within the SM ($R = 1$), certain regions of the SSM parameter space will be excluded.

Acknowledgments

N.O. thanks K. Hagiwara and the KEK Theory Group for their hospitality during his stay at KEK, where this work was completed. He also thanks the members of the CP Violation Study Group of Japan for discussions. G.C.B. thanks the CERN Theory Division for their hospitality. The work of G.C.B. was supported in part by Science Project No. SCI-CT91-0729 and EC contract No. CHRX-CT93-0132. The work of G.C.C. is supported in part by Grant-in-Aid for Scientific Research from the Ministry of Education, Science and Culture of Japan.

Appendix

The functions Y_1 and Y_2 in eqs. (11) and (14) coming from loop intergrals are given by

$$
\begin{aligned}
&Y_1(r_\alpha, r_\beta, s_i, s_j) = \\
&\quad \frac{r_\alpha^2}{(r_\beta - r_\alpha)(s_i - r_\alpha)(s_j - r_\alpha)} \ln r_\alpha + \frac{r_\beta^2}{(r_\alpha - r_\beta)(s_i - r_\beta)(s_j - r_\beta)} \ln r_\beta \\
&\quad + \frac{s_i^2}{(r_\alpha - s_i)(r_\beta - s_i)(s_j - s_i)} \ln s_i + \frac{s_j^2}{(r_\alpha - s_j)(r_\beta - s_j)(s_i - s_j)} \ln s_j, \\
&Y_1(r_\alpha, r_\alpha, s_i, s_j) = \\
&\quad \frac{r_\alpha(s_i + s_j) - 2s_i s_j}{(s_i - r_\alpha)^2(s_j - r_\alpha)^2} r_\alpha \ln r_\alpha - \frac{r_\alpha}{(s_i - r_\alpha)(s_j - r_\alpha)} \\
&\quad + \frac{s_i^2}{(r_\alpha - s_i)^2(s_j - s_i)} \ln s_i + \frac{s_j^2}{(r_\alpha - s_j)^2(s_i - s_j)} \ln s_j, \\
&Y_1(r_\alpha, r_\beta, s_i, s_i) = \\
&\quad \frac{r_\alpha^2}{(r_\beta - r_\alpha)(s_i - r_\alpha)^2} \ln r_\alpha + \frac{r_\beta^2}{(r_\alpha - r_\beta)(s_i - r_\beta)^2} \ln r_\beta \\
&\quad + \frac{(r_\alpha + r_\beta)s_i - 2r_\alpha r_\beta}{(r_\alpha - s_i)^2(r_\beta - s_i)^2} s_i \ln s_i - \frac{s_i}{(r_\alpha - s_i)(r_\beta - s_i)}, \\
&Y_1(r_\alpha, r_\alpha, s_i, s_i) = \\
&\quad - \frac{2r_\alpha s_i}{(s_i - r_\alpha)^3} \ln r_\alpha - \frac{2r_\alpha s_i}{(r_\alpha - s_i)^3} \ln s_i - \frac{r_\alpha + s_i}{(r_\alpha - s_i)^2},
\end{aligned}
$$

and

$$
\begin{aligned}
&Y_2(r_\alpha, r_\beta, s_i, s_j) = \\
&\quad \sqrt{s_i s_j}\Big[\frac{r_\alpha}{(r_\beta - r_\alpha)(s_i - r_\alpha)(s_j - r_\alpha)} \ln r_\alpha + \frac{r_\beta}{(r_\alpha - r_\beta)(s_i - r_\beta)(s_j - r_\beta)} \ln r_\beta \\
&\quad + \frac{s_i}{(r_\alpha - s_i)(r_\beta - s_i)(s_j - s_i)} \ln s_i + \frac{s_j}{(r_\alpha - s_j)(r_\beta - s_j)(s_i - s_j)} \ln s_j\Big], \\
&Y_2(r_\alpha, r_\alpha, s_i, s_j) = \\
&\quad \sqrt{s_i s_j}\Big[\frac{r_\alpha^2 - s_i s_j}{(s_i - r_\alpha)^2(s_j - r_\alpha)^2} \ln r_\alpha - \frac{1}{(s_i - r_\alpha)(s_j - r_\alpha)} \\
&\quad + \frac{s_i}{(r_\alpha - s_i)^2(s_j - s_i)} \ln s_i + \frac{s_j}{(r_\alpha - s_j)^2(s_i - s_j)} \ln s_j\Big], \\
&Y_2(r_\alpha, r_\beta, s_i, s_i) = \\
&\quad s_i\Big[\frac{r_\alpha}{(r_\beta - r_\alpha)(s_i - r_\alpha)^2} \ln r_\alpha + \frac{r_\beta}{(r_\alpha - r_\beta)(s_i - r_\beta)^2} \ln r_\beta \\
&\quad + \frac{s_i^2 - r_\alpha r_\beta}{(r_\alpha - s_i)^2(r_\beta - s_i)^2} \ln s_i - \frac{1}{(r_\alpha - s_i)(r_\beta - s_i)}\Big],
\end{aligned}
$$

$$Y_2(r_\alpha, r_\alpha, s_i, s_i) =$$
$$s_i[-\frac{r_\alpha + s_i}{(s_i - r_\alpha)^3} \ln r_\alpha - \frac{r_\alpha + s_i}{(r_\alpha - s_i)^3} \ln s_i - \frac{2}{(r_\alpha - s_i)^2}].$$

References

[1] For reviews, see e.g. I.I. Bigi, V.A. Khoze, N.G. Uraltsev, and A.I. Sanda, in *CP violation*, ed. C. Jarlskog (World Scientific, Singapore, 1989);
Y. Nir and H.R. Quinn, Ann. Rev. Nucl. Part. Sci. 42 (1992) 211;
R. Aleksan, G.C. Branco, I. Dunietz, A. Gaidot, A. Pich, and H. Steger, in Proc. of the 4th ECFA Workshop on a European B-meson Factory, Hamburg, 1993.

[2] For reviews, see e.g. H.P. Nilles, Phys. Rep. 110 (1984) 1;
P. Nath, R. Arnowitt, and A.H. Chamseddine, *Applied N=1 Supergravity* (World Scientific, Singapore, 1984);
H.E. Haber and G.L. Kane, Phys. Rep. 117 (1985) 75.

[3] Particle Data Group, Phys. Rev. D50 (1994) 1173.

[4] J. Ellis and D.V. Nanopoulos, Phys. Lett. 110B (1982) 44;
R. Barbieri and R. Gatto, Phys. Lett. 110B (1982) 211;
T. Inami and C.S. Lim, Nucl. Phys. B207 (1982) 533;
M.J. Duncan, Nucl. Phys. B221 (1983) 285;
J.F. Donoghue, H.P. Nilles, and D. Wyler, Phys. Lett. 128B (1983) 55;
A. Bouquet, J. Kaplan, and C.A. Savoy, Phys. Lett. 148B (1984) 69.

[5] L.F. Abbott, P. Sikivie, and M.B. Wise, Phys. Rev. D21 (1980) 1393.

[6] G.C. Branco, G.C. Cho, Y. Kizukuri, and N. Oshimo, Phys. Lett. B337 (1994) 316.

[7] T. Kurimoto, Phys. Rev. D39 (1989) 3447;
S. Bertolini, F. Borzumati, A. Masiero, and G. Ridolfi, Nucl. Phys. B353 (1991) 591.

[8] N. Oshimo, Nucl. Phys. B404 (1993) 20.

[9] CDF Collaboration, Phys. Rev. D50 (1994) 2966; Phys. Rev. Lett. 73 (1994) 225.

[10] The OPAL Collaboration, Phys. Lett. B337 (1994) 207.

[11] Y. Kizukuri and N. Oshimo, Phys. Rev. D45 (1992) 1806; Phys. Rev. D46 (1992) 3025.

[12] T. Inami and C.S. Lim, Prog. Theor. Phys. 65 (1981) 297.

[13] For general reviews, see e.g. J.F. Donoghue, B.R. Holstein, and G. Valencia, Int. J. Mod. Phys. A2 (1987) 319;
W. Grimus, Fortschr. Phys. 36 (1988) 201;
P.J. Franzini, Phys. Rep. 173 (1989) 1.

[14] J.R. Patterson, Plenary talk given at the 27th International Conference on High Energy Physics, Glasgow, 1994.

[15] A. Abada et al., Nucl. Phys. B376 (1992) 172;
A. Abada, LPTHE Orsay-94/57.

[16] P.B. Mackenzie, in Proc. of the XVI International Symposium on Lepton and Photon Interactions, Ithaca, 1993.

[17] W.A. Bardeen, A.J. Buras, and J.-M. Gerard, Phys. Lett. B211 (1988) 343.

[18] W.A. Kaufman, H. Steger, and Y.-P. Yao, Mod. Phys. Lett. A3 (1988) 1479;
A. Datta, J. Fröhlich, and E.A. Paschos, Z. Phys. C46 (1990) 63;
J.M. Flynn, Mod. Phys. Lett. A5 (1990) 877;
A.J. Buras, M. Jamin, and P.H. Weisz, Nucl. Phys. B347 (1990) 491;
S. Herrlich and U. Nierste, Nucl. Phys. B419 (1994) 292.

[19] G.C. Cho, Y. Kizukuri, and N. Oshimo, TKU-HEP 95/02.

[20] P. Krawczyk, D. London, R.D. Peccei, and H. Steger, Nucl. Phys. B307 (1988) 19;
C.O. Dib, I. Dunietz, F.J. Gilman, and Y. Nir, Phys. Rev. D41 (1990) 1522;
M. Lusignoli, L. Maiani, G. Martinelli, and L. Reina, Nucl. Phys. B369 (1992) 139;
A.J. Buras, M.E. Lautenbacher, and G. Ostermaier, Phys. Rev. D50 (1994) 3433;
A. Ali and D. London, CERN-TH.7398/94.

[21] J. D. Wells, C. Kolda, and G.L. Kane, Phys. Lett. B338 (1994) 219.

[22] F.M. Borzumati, Z. Phys. C63 (1994) 291.